AD-A191 142 TRANSPARENT GLASS CERAMICS DOPED BY CHROMIUM(III) AND CHROMIUM(VI) AND N..(U) HEBREW UNIV JERUSALEM (ISRAEL) DEPT OF INORGANIC AND ANALYTIC.. A REIS ET AL. 30 APR 87 DAJA45-85-C-0051 1/1

UNCLASSIFIED F/G 11/2 NL

[redacted]

END
DATE FILMED
5 88
DTIC

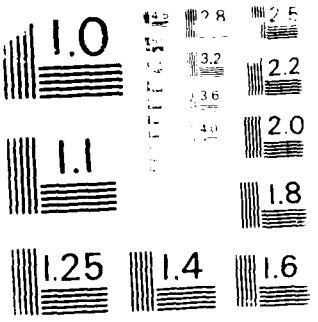
1.0
1.1
1.25
1.4
1.6
1.8
2.0
2.2
2.5
2.8
3.2
3.6
4.0

TRANSPARENT GLASS CERAMICS DOPED BY CHROMIUM(III) AND CHROMIUM(III) AND NEODYMIUM(III) AS NEW MATERIALS FOR LASERS AND LUMINESCENT SOLAR CONCENTRATORS

Research supported by U.S. Army
under contract No. DAJA 45-85-C-0051

Intermediate Report
1.10.86 - 30.4.87

Submitted by

Professor Renata Reisfeld
Department of Inorganic and Analytical Chemistry
The Hebrew University of Jerusalem
Jerusalem 91904 Israel

to

European Office of the U.S. Army
223/231 Old Marylebone Rd.
London WC1 5TH
England

and

Army Materials and Mechanics
Research Center, Watertown,
Massachusetts 02172
U.S.A.

This work was performed together with Alla Buch, Mehdi Bouderbala, Georges Boulon, Moshe Ish-Shalom, Anna Kisilev, Anne-Marie Lejus and Vincent Poncon.

CONTENTS

ABSTRACT

Transparent glass ceramics with Cr(III) were obtained by different thermal treatment of glass with composition (mol%) 73.6 SiO_2, 11.8 Al_2O_3, 4.2 Li_2O, 7.0 ZnO, 1.6 TiO_2, 1.5 ZrO_2, 0.3 As_2O_3, 0.024 Cr_2O_3, melted under various conditions. Parallel measurements of X-ray diffraction, optical and EPR spectra reveal the different formation of gahnite from precursor glass or petalite-like phase.

Laser excitation was performed for different wavelengths on Cr^{3+}-doped transparent glass-ceramics of the composition (mole%) Ac (58.7 SiO_2, 16.7 Al_2O_3, 17.8 MgO, 6.7 TiO_2, 0.03 Cr_2O_3) and Bc (49.1 SiO_2, 19.7 Al_2O_3, 21.9 MgO, 6.0 TiO_2, 3.2 ZrO_2, 0.03 Cr_2O_3), and in synthetic crystals of composition $MgAl_2O_4$ (Cr^{3+}), Mg_2TiO_4 (Cr^{3+}) and $Mg_{1.2}Ti_{0.2}Al_{1.6}O_4$ (Cr^{3+}). Analysis of the emission spectra, excitation spectra and decay curves at 4.4 K and room temperature reveals that Cr^{3+} is essentially situated on distorted single sites and in pairs exchanging Al^{3+} ions in the crystaline phase of glass ceramics.

Laser-excited emission spectra and decay curves of Cr^{3+} in gahnite-type glass-ceramics are compared with those in gahnite crystals. The nature of the Cr^{3+} sites is determined from the positions of the emission and excitation peaks and from measurements of the decay times.

CR(III) IN GAHNITE CONTAINING TRANSPARENT GLASS CERAMICS: INFLUENCE OF MELTING CONDITIONS AND HEAT TREATMENT ON CRYSTALLIZATION AND SPECTROSCOPIC PROPERTIES*

A. Kiselev and R. Reisfeld **

Department of Inorganic and Analytical Chemistry

The Hebrew University of Jerusalem, Jerusalem 91904 Israel

A. Buch and M. Ish-Shalom

Israel Ceramic and Silicate Institute

Technion City, Haifa 32000 Israel

Abstract

Transparent glass ceramics with Cr(III) were obtained by different thermal treatment of glass with composition (M%) 73.6SiO_2, 11.8Al_2O_3, 4.2Li_2O, 7.0ZnO, 1.6TiO_2, 1.5ZrO_2, 0.3As_2O_3, 0.024Cr_2O_3, melted under various conditions. Parallel measurements of x-ray diffraction, optical and EPR spectra reveal the different formation of gahnite from precursor glass or petalite-like phase.

Introduction

In a number of recent papers [1-5] unique spectroscopic properties of Cr(III) in transparent glass-ceramics were discussed. The conditions of preparation for each type of glass-ceramics were kept constant. The extent by which the conditions influence crystal formation and spectroscopic properties and reproducibility of results for given conditions is of utmost importance in designing of transparent glass-ceramics. It is the

* Supported by U.S. Army Contract No. DAJA 45-85-C-0051

** Enrique Berman Professor of Solar Energy

purpose of the present paper to examine the influence of the melting and heat treatment conditions on optical and EPR spectra of Cr(III). Further on the parallel changes of spectra and x-ray diffraction patterns are indicated.

The gahnite type ceramics in which Cr(III) has the highest quantum efficiencies was chosen for this study.

Experimental

The raw materials used for precursor glasses were sand Sibelco (99.8% SiO_2), Alcoa A-16SG (greater than 99.5 wt.% of Al_2O_3) and high purity oxides as a source for additional components.

Glasses were melted in corundum crucibles in:
1. an electrical furnace SM-12; 2. a vertical gas furnace. The melting conditions are given in Table 1. Glasses were poured into a steel mold and put in a preheated up to 650°C electrical furnace for annealing. The furnace was immediately turned off and glasses cooled at the cooling rate of the furnace.

Heat treatment of glasses was carried out in an electrical furnace. The temperature was raised at the rate of 3°-5° min^{-1}. The heat treatment temperatures and durations are given in Table 2. After heat treatment samples were cooled at the cooling rate of furnace. 10x10x3mm plates were cut and polished.

X-ray diffraction of powdered samples was done using CuKα radiation with Ni-filter in a Philips diffractometer. Repeated experiments proved the reproducibility of results.

Absorption, emission and excitation spectra and quantum efficiencies were measured as in [4].

EPR derivative spectra were taken on Varian E-12 at 9.09 GHz using

power of 10mW. Magnetic field H was varied between 500 and 4500G.

All measurements were carried out at room temperature.

Results and Discussion

The determination of crystalline phases from x-ray spectra is done by comparison with the standard tables of crystals using ASTM diffraction file, The interpretation of electronic levels from which the transition takes place is based on our previous papers dealing with spectroscopy of Cr(III) in glass ceramics [1-5]. The main conclusion is that the absorption of the first band is due to $^4A \rightarrow {}^4T_2$, the wide emission around 830nm results from $^4T_2 \rightarrow {}^4A$ distorted octahedrally Cr(III) sites at low ligand field, the narrow emission around 700nm from single Cr(III) at high field strengths [6] and the emission peaks 700-730nm are due to antiferromagnetically coupled Cr(III) pairs [1,2,7,8]. The EPR spectra in glasses are explained according to the paper of Landry et. al. [10] who performed a thorough analysis of EPR spectra of Cr(III) in glass and attribute the diffusive absorption at 1000-1500 Gauss to distorted octahedrally coordinated single Cr(III) ions [6,9 - 11]. The EPR spectra in the crystalline phase are explained by analogy with the work of Durville et. al. [9] who attribute the sharp absorption at 1580 Gauss to Cr(III) in high symmetry sites of the crystalline phase. The appearance of 1460G narrow peaks in all samples is due to the Fe(III) impurity [12].

The chemical composition of the samples prepared is identical with the previously studied gahnite glass-ceramics (M*) [1]: 73.6 SiO_2, 11.8 Al_2O_3, 4.2 Li_2O , 7.0 ZnO_2, 1.6 TiO_2, 1.5 ZrO_2, 0.3 As_2O_3, 0.024 Cr_2O_3.

While the basic composition is the same for all the samples we have changed the preparation procedure for the individual samples as detailed

in Tables 1 and 2. The numbers 1,2 and 3 in these Tables refer to the melting conditions and the subscripts to the thermal treatment.

X-ray spectra of the samples together with the previously studied sample 4 are presented in Fig. 1. The crystalline phases are listed in Table 2. Emission spectra under various excitations are shown in Fig. 2. Since the fluorescence intensities depend strongly on the nature of the crystalline phase a change in scale should be noted. Excitation maxima and corresponding quantum efficiencies are given in Table 3. Representative EPR spectra of glasses 1 and 4 and of glass-ceramics 1_1-1_3, 4, 5 (containing only β-quartz) and undoped glass and glass-ceramic are given in Fig. 3. In sample 4 the three phases gahnite, β-quartz and zirconia are crystallized in all heat treatment conditions. In contradiction in the remaining species the initial petalite phase (Fig. 1(1_1,2_1,3_1)) is transformed into gahnite with increased heat temperature (1_2-3_3) while the β-quartz remains unchanged.

The relative quantity of gahnite in each treatment can be deduced from the x-ray pattern. In the series 1_2-3_2 the highest quantity of gahnite was observed in 1_2 while in the other samples only traces of gahnite could be found. The additional heat treatment at 910°C (1_3-3_3) results in further increase in the gahnite phase. The most defined crystals are found in 1_3 (Fig. 1) while 2_3 and 3_3 reach the same amount of crystallization as 1_2.

We have shown recently that ZrO_2 with coordination number of 8 cannot incorporate Cr(III) [4]. In β-quartz both the emission (Fig. 2(1_1,2_1,3)) and EPR spectra (Fig. 3(1_1))resemble those of Cr(III) in glasses, the only difference being higher quantum efficiency which is the result of higher ligand field in the crystals as shown by the shift of $^4A_2$-$^4T_2$ absorption and emission bands to higher energies.

Of all the glass-ceramics containing gahnite we have already shown that 1_3 has the best quality crystals, and the second best being 1_2, 2_3, 3_3. These findings are also confirmed by emission and EPR spectra.

In 1_3 and to a lesser extent in 1_2, 2_3 and 3_3 the ^2E emission is characteristic by its fine structure, typical for gahnite. In 1_3 the resolution of the emission is better than in previously studied 4. In addition to these well resolved peaks around 700nm there is an additional emission at 735 due to pairs in crystalline sites [4, 13 - 15]. No $^4T_2$ emission is observed when excited at 550 nm. The structure of ^2E emission in the gahnite is more distinct in the well crystallized phase. We come to the conclusion that the previously observed $^4T_2$ emission [1] in equilibrium with ^2E arises from distorted sites but is absent when a well defined crystallization takes place. In samples 1_2, 2_3, 3_3 the crystallization is less defined, with lesser resolution of the ^2E and simultaneous presence of $^4T_2$ emission. The distribution between ^2E and $^4T_2$ is in favor of the latter in more distorted sites. A similar picture is obtained from excitation spectra. The EPR spectra are in accordance with the above optical spectra.

The highest quantum efficiency (Table 3) of 1 is obtained from ^2E in the best crystalline sites (1_3, 4). On the other hand in the distorted sites the quantum efficiencies from ^2E are lowered but from $^4T_2$ increase, indicating a thermal equilibrium between the two levels (1_2, 2_3, 3_3).

The above facts can be explained as follows: Contrary to sample 4 which was prepared in an electrical oven in small quantity (100 gr) the samples discussed in the present work were melted in a furnace in much larger quantities(1000 gm).It is therefore the heat capacity which influences the rate of cooling, heating and temperature gradient which decides the thermal history. That the atmosphere is not reducing is concluded from the absence of Ti(III) [16,17]. In the first step the glass is formed,

which after heating to 750°C undergoes phase separation. Under additional heat treatment the glassy phase rich in SiO_2 forms β-quartz, while the phase in which the concentration of cations prevails forms a thermodynamically metastable petalite-like phase. The latter after further heat treatment undergoes a change to the more stable gahnite phase. Both petalite and ghanite are rich in cations. Since gahnite is formed here from the crystalline phase, the crystallization is more defined and quality of crystals is better than in the ghanite [4]. Remelting improves the glass [1] uniformity which is reflected in compositional changes of coexistent phases after heat treatment [2,3]. The new petalite phase is then richer in silica and subsequent ghanite formation more difficult.

It is worthwhile noting that β-quartz appears in larger quantities than gahnite, however the emission of Cr(III) and the EPR spectra shows that the concentration of Cr(III) is much higher in the latter. This is further evidenced by appearance of Cr(III) pairs which are known to appear at high concentration [9, 10]. It has been shown [9, 12] that Cr(III) may serve as nucleator for gahnites and related spinels where it enters the crystalline sites replacing aluminum. This situation is thermodynamically preferred to Cr(III) in β-quartz where it can enter only at interstitial sites.

Conclusions

1. The crystallization processes in the gahnite glass-ceramics depend on the heat treatment schedule as well as on the thermal history of the precursor glasses.
2. The spectroscopic properties depend on the type and quality of the crystalline phases.

3. The structure of the ^2E emission depends exclusively on the quality of the gahnite crystals. The ratio of emissions from $^4T_2$ and ^2E levels in glass-ceramics is determined by relative distribution of Cr(III) ions between the β-quartz and distorted crystalline gahnite sites and the undistorted crystalline sites.
4. The quantum efficiency of Cr(III) strongly increases upon crystallization processes, reaching the value of 1.0 in the well-developed gahnite glass-ceramics.

Acknowledgements

The authors are grateful to Dr. M. Eyal for his great help in computer processing of experimental data, and to Dr. H. Ofir for her kind help in EPR measurements.

References

1. R. Reisfeld, A. Kiselev , E. Greenberg , A. Buch and M. Ish-Shalom , Chem. Phys. Lett. 104 (1984) 153.
2. A. Kiselev, R. Reisfeld, E. Greenberg , A. Buch and M. Ish-Shalom , Chem. Phys. Lett. 105 (1984) 405.
3. A. Buch , M. Ish-Shalom, R. Reisfeld, A. Kiselev and E. Greenberg , Mater. Sci. and Eng. 71 (1985) 383.
4. A. Kiselev and R. Reisfeld, Non-cryst. Solids in press.
5. M. Bouderbala , G. Boulon , R. Reisfeld, A. Buch , M. Ish-Shalom and A.M. Lejns , Chem. Phys. Lett. 121 (1985) 535.
6. S. Sagano , Y. Tanabe and H. Kamamura , "Multiplets of Transition-Metal Ions in Crystals ," Academic Press New York , 1970.
7. R. Reisfeld in Electronic Structure of New Materials Report Swedish Academy of Engineering Sciences in Finland , 40 (1984) 7.
8. R. Reisfeld , Mater. Sci. and Eng 71 (1985) 375.
9. F. Durville , B. Champagnon , E. Duval and G. Boulon , J. Phys. Chem. Solids , 46 (1985) 701.
10. R.J. Landry , J.T. Fournier and C.G. Young J. Chem. Phys. 46 (1967) 1285.
11. R.H. Clarke , L.J. Andrews and H.A. Frank , Chem. Phys. Lett. 85 (1982) 161.
12. R.S. Abdrakhmanov , E.M. Konoval and I.V. Shishkin , Fizika i Khimiya Stekla , 9 (1983) 403.
13. J. Derkosch , W. Mikenda and A. Preisinger , Spectrochim. Acta 32A (1976) 1759.
14. W. Mikenda and A. Preisinger J. Lumin. 26 (1981) 53.
15. W. Mikenda and A. Preisinger J. Lumin. 26 (1981) 67.
16. H.M. Pavlushkin , R.Ya. Chodakovskaya, L.A. Orlova , V.V. Orlov , Neorganitcheskie Materiali 10 (1974) 1952 (in Russian).
17. N.R. Yafaev and Yu.V. Yablokov , Fizika Tverdogo Tela , 4 (1962) 1529.

TABLE 1

Melting Conditions of Glasses

Assignment	melting, furnace	amount, g	Heating time, h, to 1580° (1600°)	melting temperature °C	melting time, h	remelting i the electri cal furnace at 1560° time, h
4	electrical	100	10	1580	2	-
1	gas	1000	4	1600	3.5	-
2	gas	1000	4	1600	3.5	1.5
3	gas	1000	4	1600	3.5	5

Table 2

Heat treatment conditions and crystalline phases in gahnite containing transparent glass-ceramics.

Assignment	Heat Treatment						crystalline phases	outward appearance color	Pefractive index
	Nucleation		Crystallization						
	Temp. (°C)	Soaking time (h)	Temp. (°C)	Soaking time (h)	Temp. (°C)	Soaking time (h)			
4	750°	10	860°	2	-	-	β-quartz ss ZrO_2 (T) gahnite	greyish-green transparent	1.56
1_1 2_1 3_1	750°	10	860°	2	-	-	β-quartz ss petalite-like phase ZrO_2 (T)	yellowish-green transparent	1.545
1_2							β-quartz ss ZrO_2 (T) gahnite	greenish-rose transparent	1.55
2_2	750°	10	860°	2	890°	2	β-quartz ss ZrO_2 (T) gahnite (traces)	yellowish-green transparent	1.545
3_2							β-quartz ss ZrO_2 (T) gahnite (traces)	yellowish-green transparent	1.545
1_3								rose transparent	1.565
2_3	750°	10	900°	1.5	910	2	β-quartz ss ZrO_2 (T) gahnite	greenish-rose transparent	1.55
3_3								greenish-rose transparent	1.55

TABLE 3

Quantum Efficiencies and Excitation Maxima of Cr(III) in Unheat-treated Glasses and Gahnite Containing Transparent Glass-ceramics.

Sample		Emission		Excitation	
Assignment		Wavelength of excitation, λ, nm	Quantum Efficiency, η	Wavelength of emission, λ, nm	Excitation maxima *
4	glass	625	0.13	850	∿625 vw
	glass-ceramics	620	0.34	830	∿620 vw
				695	545 + 620 s
		525	1.0	705	
1	glass	625	0.10	850	∿625 vw
1_1	glass-ceramics	625	0.30	850	∿620 vw
				785	
1_2	glass-ceramics	625	0.92	775	540 + 615
				735	530 + 615 s
		530	0.55	675	530
1_3	glass-ceramics	617	0.62	780	545 + 620
				735	530 + 620 s
		525	1.0	695, 671	520
2	glass	625	0.10	850	∿625 vw
2_1	glass-ceramics	625	0.25	830	∿620 vw
2_2	glass-ceramics	625	0.32	830	∿620 vw
		560	0.56	707	560 + 620 e
2_3	glass-ceramics	625	0.75	780	550 + 615 e
		540	0.89	705	540 + 615 s
3	glass	625	0.05	850	∿625 vw
3_1	glass-ceramics	625	0.3	830	∿620 vw
				707	560 + 620
3_2	glass-ceramics	625	0.45	810	∿615 vw
		550	0.55	707	550 + 615 e w
3_3	glass-ceramics	625	0.60	800	540 s + 615 vw
				750	540 + 610 s
		540	0.60	705	540 + 610 s

* vw - very wide, s - small, e - equal (540 ∿ 625)

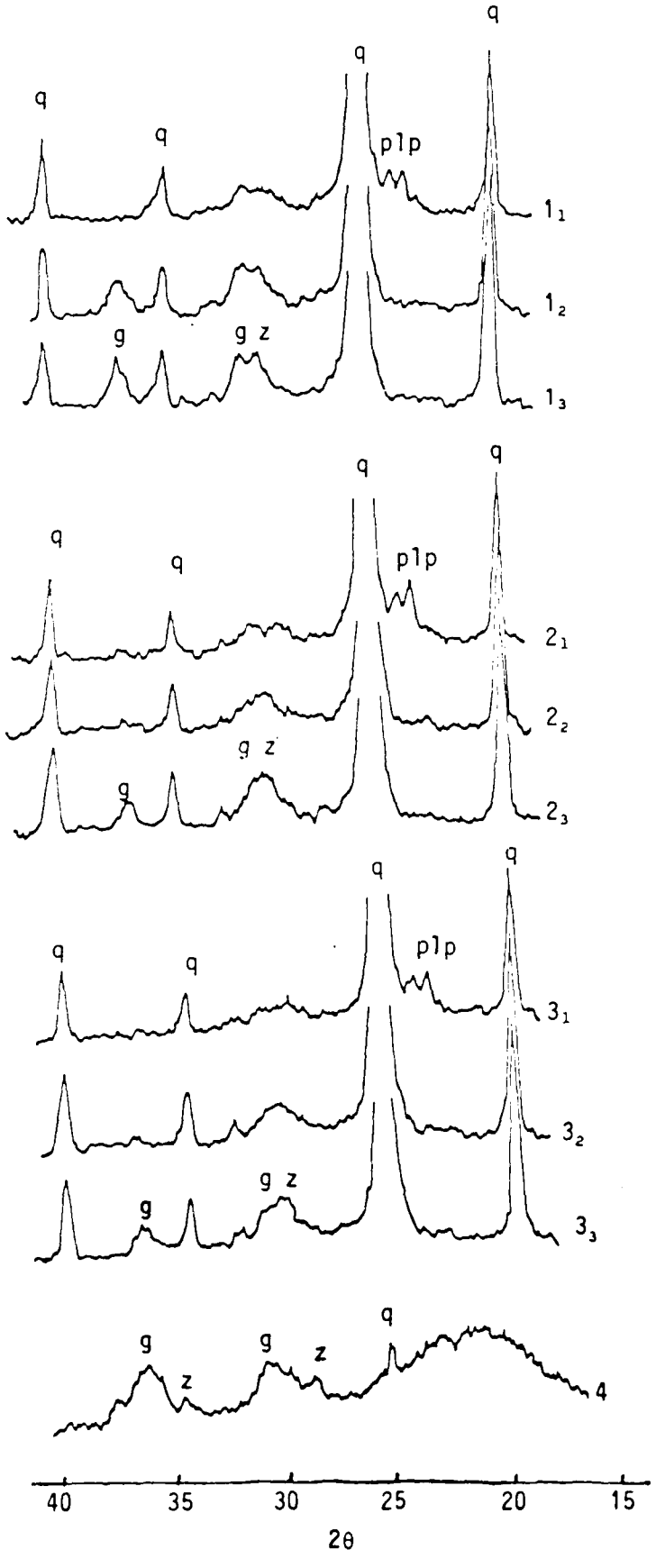

Fig. 1. X-ray diffraction spectra of the gahnite containing transparent glass-ceramics depending on melting conditions and subsequent heat treatment.

q - β-quartz SS
plp - petalite like phase
g - gahnite
z - ZrO_2

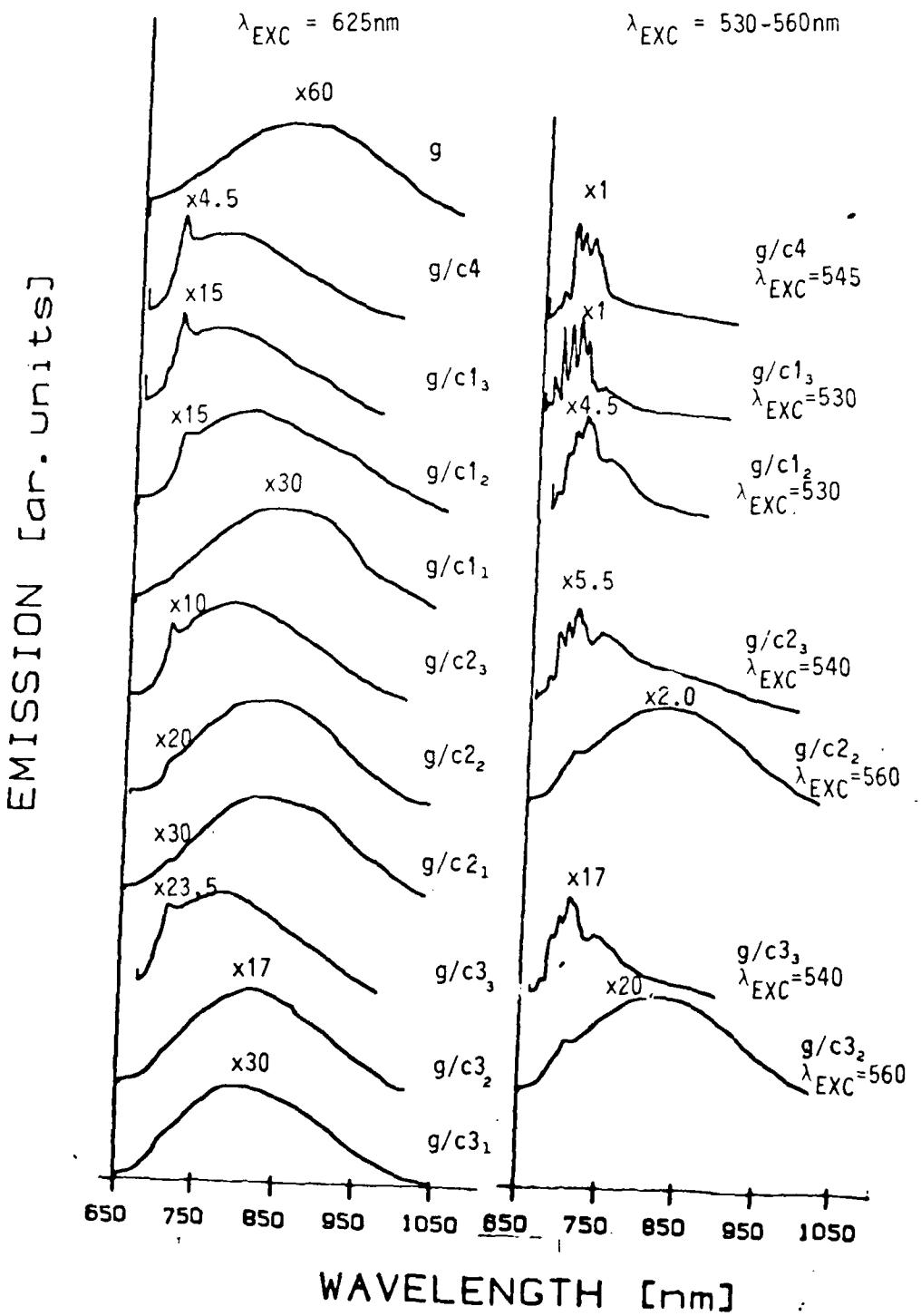

Fig. 2. Emission spectra of Cr(III) doped gahnite containing glass-ceramics
g - glass, g/c - glass-ceramics

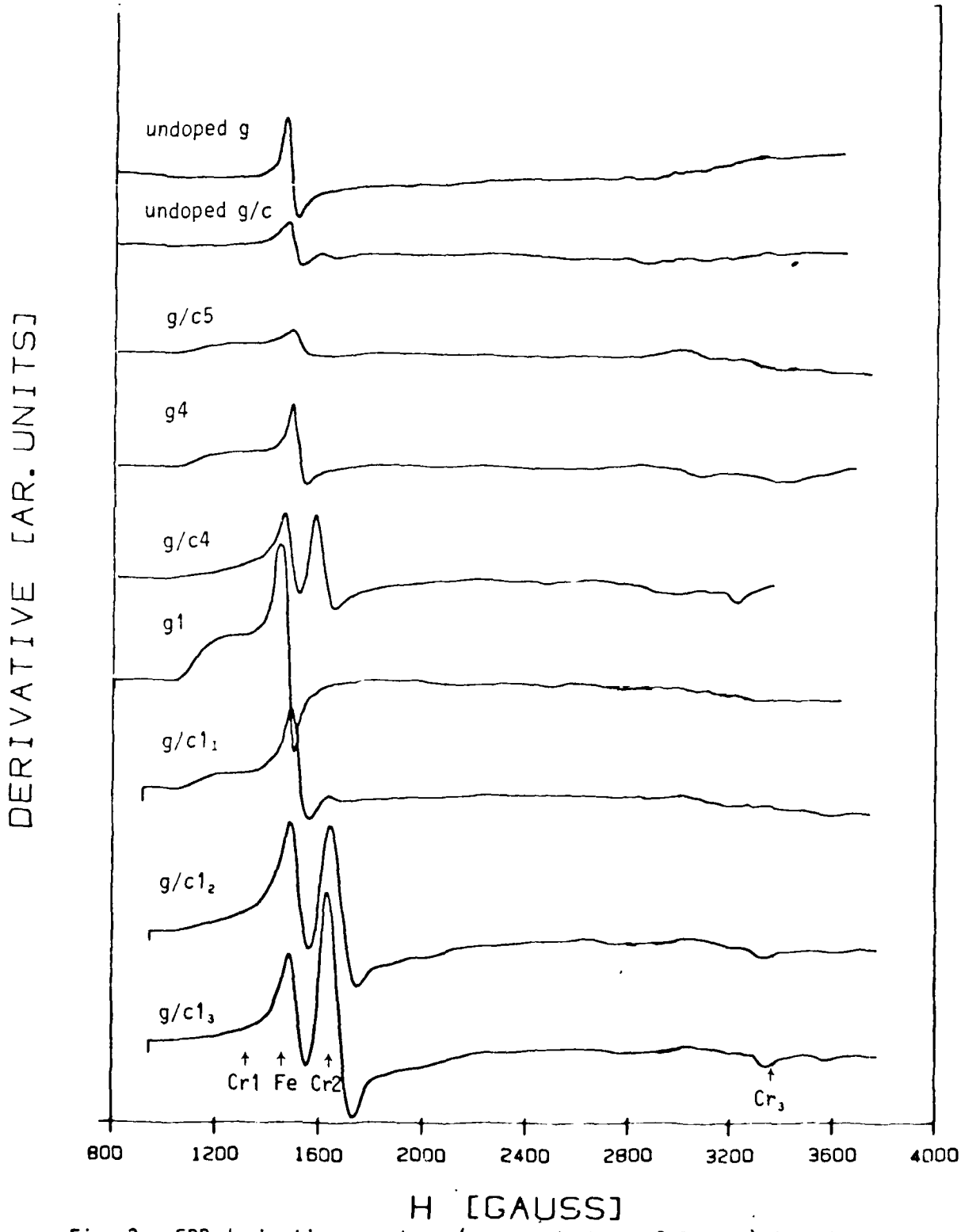

Fig. 3. EPR derivative spectra (measured at ν = 9.09G Hz) in unheat-treated glasses and gahnite containing glass-ceramics.
g - glass; g/c - glass-ceramics. Cr1 - Cr(III) in glassy phase; Cr2 - Cr(III) in gahnite phase; Cr3 - Cr(III) exchanged-coupled pairs.

LASER-SPECTROSCOPY OF Cr^{3+} IN MAGNESIUM ALUMINATE SPINELS AND TRANSPARENT GLASS-CERAMICS*

Mehdi Bouderbala, Georges Boulon
Laboratoire de Physico-Chimie des Materiaux Luminescents
Universite Claude Bernard Lyon-Unite associee au CNRS
69622 - Villeurbanne, France

Anne-Marie Lejus
Laboratoire de Chimie Appliquee del'Etat Solide
Ecole Nationale Superieure de Chimie de Paris
Universite Pierre et Marie Curie.
Unite associee au CNRS, 75231 Paris, France

Anna Kisilev, Renata Reisfeld**
Department of Inorganic and Analytical Chemistry
The Hebrew University of Jerusalem, Jerusalem 91904, Israel

Alla Buch, Moshe Ish-Shalom
Israel Ceramic and Silicate Institute
Technion City, Haifa 32000, Israel

Laser excitation was performed for different wavelengths on Cr^{3+} doped transparent glass-ceramics of the composition Ac (58.7 SiO_2; 16.7 Al_2O_3; 17.8 MgO; 6.7 TiO_2; 0.03 Cr_2O_3) and Bc (49.1 SiO_2; 19.7 Al_2O_3; 21.9 MgO; 6.0 TiO_2; 3.2 ZrO_2; 0.03 Cr_2O_3) and in synthetic crystals of the composition $MgAl_2O_4$ (Cr^{3+}), Mg_2TiO_4 (Cr^{3+}) and $Mg_{1.2}Ti_{0.2}Al_{1.6}O_4$ (Cr^{3+}). The analysis of the emission spectra, excitation spectra and decay curves at 4.4 K and room temperature reveals that Cr^{3+} is essentially situated on distorted single sites and pairs exchanging Al^{3+} ions in the crystalline phase of glass-ceramics.

---

* Partially supported by U.S.Army contract DAJA 45-85-C-0051.

** Enrique Berman Professor of Solar Energy.

1. INTRODUCTION

We have recently studied a variety of Cr^{3+} doped transparent glass-ceramics in view of their importance as possible materials for tunable lasers and luminescent solar concentrators [1-4]. The x-ray spectra provide us with information about the type of the main crystallite phases [5]. However in order to obtain a more detailed insight into the nature of the emitting Cr^{3+} sites a comparison of the optical spectra and decay dynamics between the transparent glass-ceramics and crystallites is needed. Detailed studies of the steady state spectroscopy of Cr^{3+} in natural spinel crystals and related powdered samples have been performed by Mikenda and al [6-9]. The authors have observed the R-line of Cr^{3+}, which is intense at low Cr^{3+} concentration, disappears gradually with increase of Cr^{3+} concentration and is replaced by a number of lines due to different groups of Cr^{3+} ions such as pairs, agglomerates and distorted single ions with the increase in the degree of inversion.

In the present study we have prepared crystals of $MgAl_2O_4$, Mg_2TiO_4 and $Mg_{1.2}Ti_{0.2}Al_{1.6}O_4$ doped by 0.1 to 1% Cr^{3+}. The steady state emission at various excitations and temperatures as well as the decay of fluorescence of these samples and of transparent glass-ceramics Ac (58.7 SiO_2; 16.7 Al_2O_3; 17.8 MgO; 6.7 TiO_2 doped by 0.03 Cr_2O_3 and Bc (49.1 SiO_2; 19.7 Al_2O_3; 21.9 MgO; 6.0 TiO_2; 3.2 ZrO_2 doped by 0.03 Cr_2O_3) have been studied [10]. The crystallography of x-ray analysis of sample Ac reveals the main spinel type phase and Bc the main petalite type phase [5].

In addition to the knowledge gained from the optical properties, the type of study described here is of importance in determining the nucleation kinetics [11-13].

2. EXPERIMENTAL TECHNIQUES

Polycrystalline samples of Mg_2TiO_4 doped by 1 wt % of Cr^{3+} were obtained by coprecipitation of stoichiometric quantities of magnesium and chromium nitrates and titanium chloride with ammonia. The precipitate was heated to 350°C and disks were pressed from the corresponding powders and sintered at 1550°C followed by annealing.

The $Mg_{1.2}Ti_{0.2}Al_{1.6}O_4$ samples doped by 0.1 and 1 wt % of Cr^{3+} were obtained in a similar way by precipitation with the addition of stoichiometric quantities of aluminium hydroxide.

The $MgAl_2O_4$ samples containing 1 wt % of Cr^{3+} were sintered at 1100°C.

The dimensions of the a parameter in the cubi spinel measured by x-ray diffraction are as follows:

a = 8.08 Å for $MgAl_2O_4$

a = 8.16 Å $Mg_{1.2}Ti_{0.2}Al_{1.6}O_4$

a = 8.44 Å Mg_2TiO_4

The optical measurements were made by using an experimental set-up described in reference [14]. The laser was a Quantel YAG-Nd pulsed laser followed by a tunable dye-laser (repetition rate: 10 Hertz. time-constant: 15 ns) to scan the required wavelength. The decay curves were recorded using a multichannel analyser Intertechnique IN 90 with a resolution of 2 µs.

3. RESULTS AND DISCUSSION

a. Emission spectra

The emission spectra under 590 nm excitation due to the $^4A_2$ --> $^4T_2$ transition for crystalline samples and glass-ceramics are presented in Figure 1-a at room temperature and in Figure 1-b at 4.4 K. We can see in all cases that the emission peak at longer wavelengths is more intense at lower temperatures. The R-lines at 684.8 nm observed by Mikenda in spinel samples due to regular octahedral sites are absent in our samples. This indicates that the single Cr^{3+} ions are positioned in distorted symmetry sites peaking at 688.2 nm and 691.8 nm. The additional peak around 705 nm is due to pairs assigned to N_4 by Mikenda et al.[6] As expected the concentration is increased for pairs at lower temperatures as evidenced by the increase of the peak around 70-5 nm at 4.4 K.

The spectra of Ac and Bc glass-ceramics are similar to the mixed compound $Mg_{1.2}Ti_{0.2}Al_{1.6}O_4$ and $MgAl_2O_4$ but do not resemble the Mg_2TiO_4. No peak characteristic for Mg_2TiO_4 is detected. We can therefore assume that the Cr^{3+} replaces the Al^{3+} in the octahedrally distorted sites in the crystalline phase with a large degree of inversion. The peak at around 705 nm in the mixed compound which was also detected by x-ray in the glass-ceramics can be due either to more distorted ions or pairs, the intensity of which is higher at low temperature as was mentioned above.

In the Mg_2TiO_4 sample the emission peak of Cr^{3+} is shifted to longer wavelengths indicating that Cr^{3+} is subjected to a lower ligand field, smaller Dq value and the ^2E and $^4T_2$ levels are

closer than in $MgAl_2O_4$ so that $^4T_2$ --> $^4A_2$ emission may occur. But the exact position of Cr^{3+} (substitutional or interstitial ctahedral sites) is not known.

In addition the time resolved spectra of glass-ceramics under longer wavelengths (680, 684 and 690 nm) at room temperature show that the broad band observed in this case is essentially due to $^4T_2$ --> $^4A_2$ transition as can be seen in Figure 2.

b. Excitation Spectra

The excitation spectra for the various emissions of Cr^{3+} in glass-ceramics Ac and Bc are exactly the same. They are presented in Figure 3. They arise from $^4A_2$ --> $^4T_2$ transition which is different for different sites situated at a different ligand field. The shortest wavelength corresponds to the highest value of the Dq parameter which is similar in ruby [1]. By monitoring the ^2E --> $^4A_2$ fluorescence at 686.1 and 696.1 nm (distorted single ions), 704.6 nm (pairs and distorted single ions) and the $^4T_2$ $^4A_2$ fluorescence at 790.6 nm (Cr^{3+} doped glassy phase and Mg_2TiO_4 compound), constituents of the $^4A_2$ --> $^4T_2$ transition have a maximum at respectively: 544, 555, 559, and 620 nm. We note also the evidence of energy transfer between the distorted single Cr^{3+} and pairs.

4. DECAY MEASUREMENTS

Figure 4 presents the decay profiles on a semilog scale for Cr^{3+} ions in glass-ceramics Ac and Bc, spinel $MgAl_2O_4$ and $Mg_{1.2}Ti_{0.2}Al_{1.6}O_4$ at room temperature under 590 nm excitation. The measurements were made for distorted sites at 688.2 and 691.8 nm and for 715.7 nm which coincides with the peak of Mg_2TiO_4. The decay profiles at 4.4 K have already been presented in reference [10].

No significance differences were found in the shapes of decay profiles between 4.4 K and room temperature for glass-ceramics Ac and Bc. However the long portion corresponds to a slightly longer time constant from 10 ms at room temperature to 13.5 ms at 4.4 K (Figure 3-a of reference [10]). In crystalline spinel the decay is almost exponential with only a small deviation at very short lifetimes. In glass-ceramics the deviation from exponentiality is much stronger, the exponential portion appearing only at longer lifetimes. The nonexponential part of the decay curve requires additional analysis in connection with the presence of multisites and the energy transfer mechanisms between them.

The longest time-constant of τ =13 ms is detected for Cr^{3+} ions in spinel situated at almost regular octahedral symmetry. The single ions emitting at 688.2 nm and 691.8 nm in Ac and Bc glass-ceramics with longer decay times have a higher transition probability of emission since they are situated in more distorted sites. The distortion of the mixed compound is even greater. For the pairs emitting at 715.7 nm the situation is similar in glass-ceramics and in the mixed compound at longer time but not at shorter time. The shortest time constant is obtained in Mg_2TiO_4 (τ = 0.8 ms) with a strong deviation from the exponential at the beginning of the decay. It is probably the result of energy transfer between Cr^{3+} ions in the low ligand field sites and pairs and the evidence of $^4T_2$ emission along with the ^2E emission.

The general exponential behaviour of the decay curves at longer times may be interpreted by the emission of long lived sites of the same nature to which energy has been transferred from the ^2E level of other sites. As mentioned above the decay curves mainly reflect the ^2E emission. However at short times some $^4T_2$ emission may be hidden: it is very clear in the case of Mg_2TiO_4.

In this way we do not have a random distribution of Cr^{3+} ions and also have shown that the samples contain a great variety of sites with different ligand field strengths. Therefore the interpretation of the decay kinetics needs a more refined treatment taking into account the various types of interaction [15].

5. CONCLUSION

The nature of the emitting sites can be detected from different emission spectra at various excitation wavelengths. The absence of the R-line is evidence that no undistorted sites are present in glass-ceramics and synthetic spinel. The distortion is the highest in Mg_2TiO_4 crystal with the longest emission wavelength. The distributiuon of Cr^{3+} ions in various phases favors the $MgAl_2O_4$ in the spinel type glass-ceramics. Energy transfer occurs between the short-lived and the long-lived sites both in glass-ceramics and in crystals. The simultaneous emission from $^4T_2$ and ^2E states in distorted sites of the glass-ceramics make them a good potential material for tunable lasers [1].

Acknowledgement: The authors are very grateful to Dr. M. Eyal for fruitful discussions and also to Mr. and Mrs. Willy Berler for their kind support of the work at the Hebrew University.

REFERENCES

1. R. Reisfeld, Materials Science and Engineering 71 (1985) 375.
2. R. Reisfeld, A. Kisilev, E. Greenberg, A. Buch and M. Ish-Shalom. Chem. Phys. Letters 104 (1984) 153.
3. A. Kisilev, R. Reisfeld, E. Greenberg, A. Buch and M. Ish-Shalom. Chem. Phys. Letters 104 (1984) 405.
4. A. Buch, M. Ish-Shalom, R. Reisfeld, A. Kisilev and E. Greenberg. Materials Science and Engineering 71 (1985) 383.
5. A. Kisilev, R. Reisfeld, A. Buch and M. Ish-Shalom. J. Noncryst. Solids (to be published).
6. W. Mikenda and A. Preisinger. J. Luminescence 26 (1981) 53.
7. W. Mikenda and A. Preisinger. J. Luminescence 26 (1981) 67.
8. W. Mikenda. J. Luminescence 26 (1981) 85.
9. J. Derkosh and W. Mikenda. J. Luminescence 28 (1983) 431.
10. M. Bouderbala, G. Boulon, R. Reisfeld, A. Buch, M. Ish-Shalom and A.M. Lejus. Chem. Phys. Letters 121 (1985) 535.
11. F. Durville, B. Champagnon, E. Duval, G. Boulon, F. Gaume, A.J. Wright and A.N. Fitch. Phys. Chem. Glasses 25 (1984) 126.
12. F. Durville, B. Champagnon, E. Duval and G. Boulon. J. Phys. Chem. Solids 46 (1985) 701.
13. B. Champagnon, F. Durville, E. Duval and G. Boulon. J. Luminescence 31-32 (1984) 345.
14. G. Boulon. Energy Transfer Processes in Condensed Matter (ed. B. Di Bartolo) - Plenum Press (1983). ASI Series - Series B: Physics 114 (1984) 603.
15. D. Huber. Laser Spectroscopy of Solids (ed. W.M. Yen and P.M. Selzer) Springer-Verlag, Berlin 49 (1981) 83.

FIGURE CAPTIONS

Figure 1. Emission spectra of different samples under 590 nm laser excitation: a - room temperature; b - 4.4 K

Figure 2. Time resolved spectra of spinel type glass-ceramics (Ac) excited at 680 nm at room temperature. The gate width was 100 μs. D is the time delay.

Figure 3. Excitation spectra of different samples in the $^4A_2$ $^4T_2$ spectral range by monitoring fluoride emission λ_{em}. (T = 4.4 K).

Figure 4. Decay curves of the fluorescence λ_{em} on semilog scale for different samples at room temperature.

Fig 1

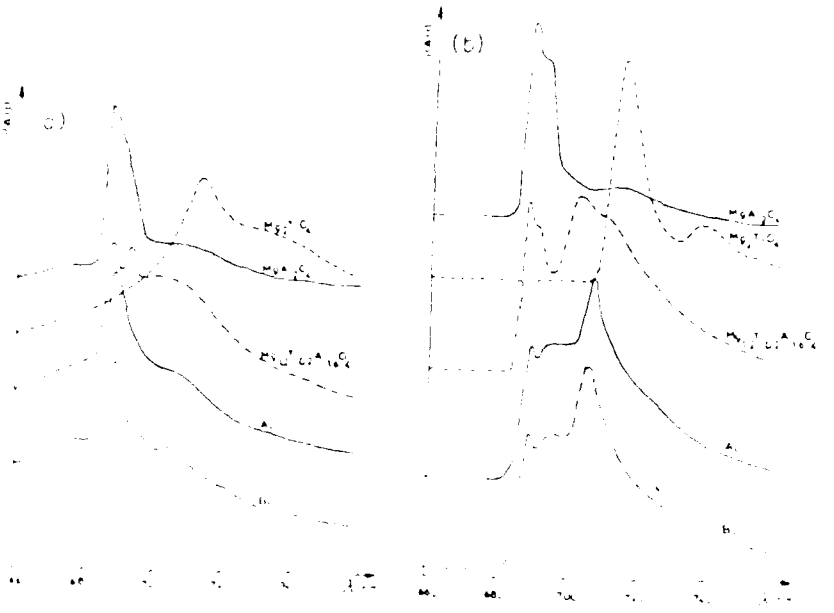

Fig 2

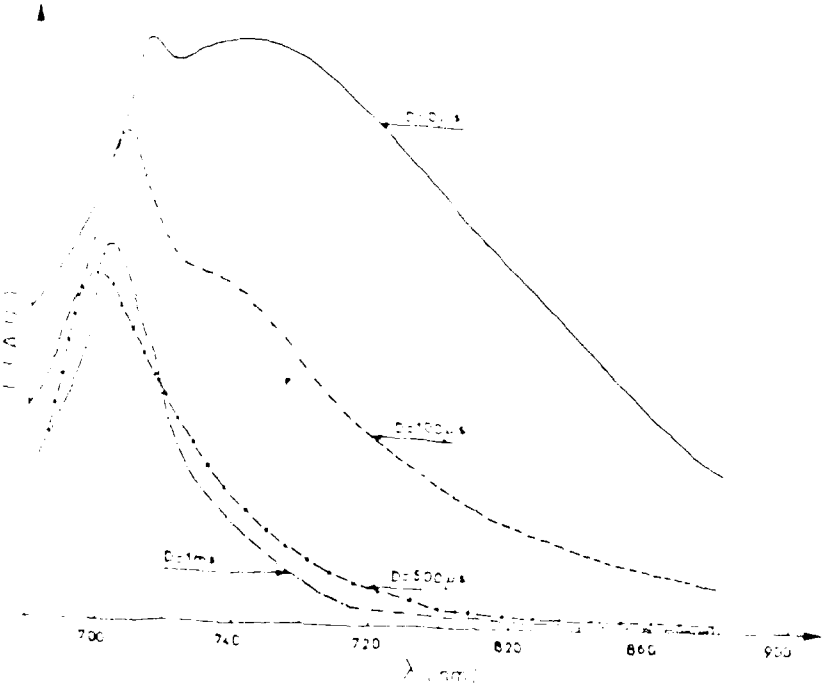

Fig 3.

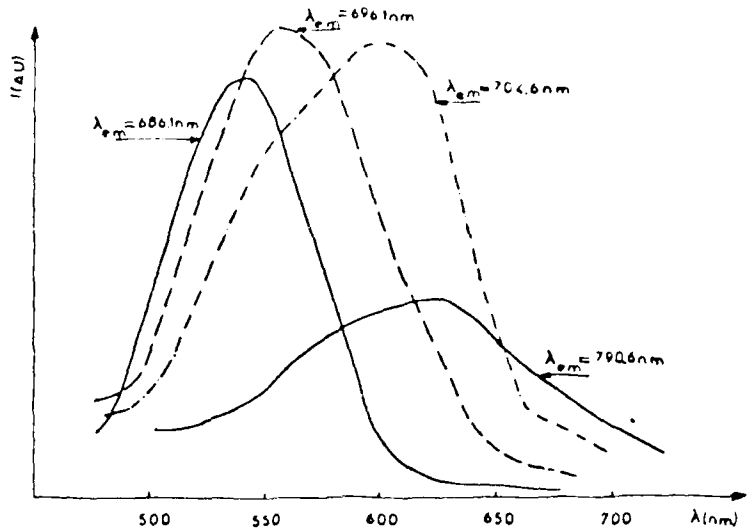
I(a.u)
λem=696.1nm
λem=704.6nm
λem=688.1nm
λem=719.6nm
500
550
600
650
700
λ(nm)

Fig 4

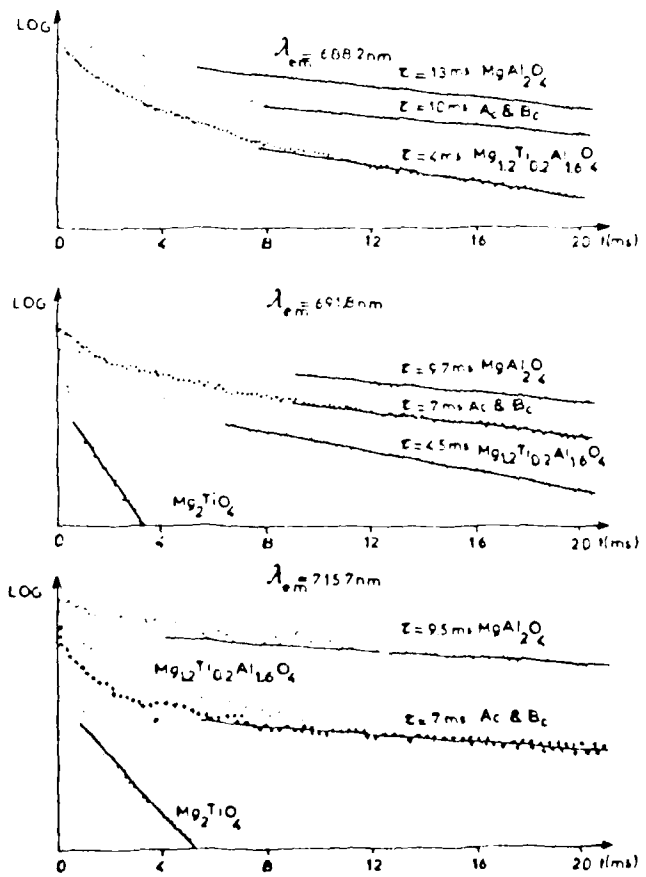
LOG
λem=688.2nm
τ=13ms MgAl2O4
τ=10ms Ac & Bc
τ<4ms Mg1.2Ti0.2Al1.6O4
0
4
8
12
16
20 t(ms)
LOG
λem=691.8nm
τ=9.7ms MgAl2O4
τ=7ms Ac & Bc
τ<4.5ms Mg1.2Ti0.2Al1.6O4
Mg2TiO4
0
4
8
12
16
20 t(ms)
LOG
λem=715.7nm
τ=9.5ms MgAl2O4
Mg1.2Ti0.2Al1.6O4
τ=7ms Ac & Bc
Mg2TiO4
0
4
8
12
16
20 t(ms)

LASER SPECTROSCOPY OF Cr^{3+} IN GAHNITE CRYSTAL AND TRANSPARENT GAHNITE-TYPE GLASS-CERAMICS*

Vincent Poncon[**], **Mehdi Bouderbala, Georges Boulon**
Laboratoire de Physico-Chemie des Materiaux Luminescents
Universite Claude Bernard Lyon - Unite associee au CNRS
69622 Villeurbanne France.

Anne-Marie Lejus
Laboratoire de Chimie Appliquee de l'Etat Solid
Ecole Nationale Superieure de Chimie de Paris
Universite Pierre et Marie Curie, Unite associee au CNRS
75231 Paris, France

Renata Reisfeld[#]
Department of Inorganic and Analytical Chemistry
The Hebrew University of Jerusalem
Jerusalem 91904, Israel

Alla Buch and Moshe Ish-Shalom
Israel Ceramic and Silicate Institute, Technion City
Haifa 32000, Israel

ABSTRACT

Laser excited emission spectra and decay curves of Cr^{3+} in gahnite-type glass-ceramics were compared with those in gahnite crystals. The nature of the Cr^{3+} sites is determined from the positions of the emission and excitation peaks and from the measurements of the decay times.

* Partially supported by US Army Contract DAJA 45-85-C-0051.

** Saint Gobain Recherche

Enrique Berman Professor of Solar Energy.

1. INTRODUCTION

We have studied recently the spectroscopy of Cr^{3+} in gahnite-type glass-ceramics of the composition 70.2 SiO_2; 15.0 Al_2O_3; 4.4 ZnO; 7.1 Li_2O; 1.5 TiO_2; 1.5 ZrO_2; 0.3 As_2O_3 doped by Cr^{3+} at a concentration of 1.1×10^{19} ions/cm^3 and found very high quantum efficiency of the $^2E \rightarrow {}^4A_2$ and $^4T_2 \rightarrow {}^4A_2$ emissions. The emission from $^4T_2$ at room temperature in gahnite when excited at 625 nm can arise either from the glassy phase or the crystalline phase in which the $^4T_2$ is of equal or slightly higher energy than the ^2E level. The simultaneous emission of ^2E and $^4T_2$ is important for designing tunable lasers based on broad Cr^{3+} emission [1,2]. In the present paper we have introduced Cr^{3+} into gahnite crystals and the Cr^{3+} spectroscopy of these crystals is compared with that of gahnite-type glass-ceramics. The temperature dependence of the emission and the decay curves allow us to identify the levels and the nature of sites from which the emissions take place.

2. EXPERIMENTAL

The gahnite glass-ceramics samples were prepared from a glass of starting composition 70.2 SiO_2, 15.0 Al_2O_3, 4.4 ZnO, 7.1 Li_2O, 1.5 TiO_2, 1.5 ZrO_2, 0.3 As_2O_3 mole % as described in reference 3. The glasses were doped by Cr^{3+} at a concentration of 1.1×10^{19} ions/cm^3.

Powdered crystalline samples of Cr^{3+} doped $ZnAl_2O_4$ gahnite were prepared from stoichiometric ratios of $Zn(NO_3)_2$, $Cr(NO_3)_3$ and $Al(NO_3)_3 \cdot 9H_2O$ precipitated by ammonium hydroxide. The precipitate was heated at 400 °C and then disks pressed and sintered for 48 hours at 1100 °C.

The lattice constant a of the crystalline $ZnAl_2O_4$ was found by X-rays to be 8.085 Å.

The optical measurements were made using an experimental set-up described in reference 4. The laser was a Quantel YAG-Nd pulsed laser followed by a tunable dye-laser (repetition rate - 10 Hertz, time constant - 15 ns) to scan the required wavelength. The decay curves were recorded using a multichannel analyzer Intertechnique IN 90 with a resolution of 2 μs.

3. RESULTS AND DISCUSSION

Figures 1a and 1b present a comparison of the emission spectrum of Cr^{3+} in $ZnAl_2O_4$ excited at 532 nm which is the maximum absorption peak due to $^4A_2$ --> $^4T_2$ transition in this material and of Cr^{3+} in gahnite-like glass-ceramics at various excitation wavelengths at 4.4 K. We observe the R_1-line of Cr^{3+} at 686.2 nm both in $ZnAl_2O_4$ crystal and in glass-ceramics in contrast with $MgAl_2O_4$ synthetic crystal and glass-ceramics where no such line appears [5]. The appearance of these lines is an evidence of Cr^{3+} in almost octahedral symmetry with no inverted site by analogy with the work of Mikenda et al [6]. The N_1 (688.6 nm) line seen clearly both in

the crystal and in glass-ceramics is actually ascribed to distorted Cr^{3+} sites. N_2 (692.3 nm) has much lower intensity than N_1 and is seen clearly in the crystal but it obscured in the glass-ceramics. X (~697.0 nm) is of comparable intensity with the N_1 line in the crystal and lower than the N_1 line in glass-ceramics. It has been shown by Mikenda to decrease with the concentration of Cr^{3+} ions [6]. Therefore it has to be ascribed to singly perturbed ions. N_4 group of lines (705.0 to 715.0 nm) can be ascribed to distorted Cr^{3+} pairs. In the crystal three distinct lines can be seen and one broad band in the glass-ceramics as evident from Figure 1b. The intensity of these bands increases at lower temperature due to increased association of Cr^{3+} into pairs. The existence of the pairs was also seen by EPR measurements [7].

The excitation spectra due to $^4A_2$ --> $^4T_2$ transition of the various emissions at 4.4 K are presented in Figure 2. The excitation peaks shift to lower energies in the order from:

R_1-line (686.2 nm)

N_1-line (688.6 nm)

X-lines (701.2 nm)

$^4T_2$ --> $^4A_2$ band (730.6 nm)

$^4T_2$ --> $^4A_2$ band (790.6 nm)

which is consistent with the fact that the more regular Cr^{3+} sites are subjected to higher, and the pairs to the lower, field strengths.

Figure 3 shows the time dependence of the emission spectra at 4.4 K under 570 nm excitation. The R-line has the longest time-constant, the pairs exhibit the shortest time-constant as expected,

while the perturbed ions are the intermediate case. This fact is also evident from Figs. 4a and 4b. The decay times of Cr^{3+} in $ZnAl_2O_4$ are presented in Figure 4a-B and C, and of gahnite-type glass-ceramics in Figure 4a-A and Figure 4b-A-B-C. The slopes of the semilog curves for the crystal are exponential in most cases, with slight deviation of the exponentiality at very short times. In the glass-ceramics the deviation from exponentiality occurs at much longer time intervals The decay time constants may be obtained from the exponential portions of the curves in Figure 4. The extremely long life-time of 33 ms in the crystal at 4.4 K is indicative of the very high symmetry in which Cr^{3+} is situated. It also results from energy transfer from the R-line to pairs and to perturbed ions. The fact that the long time portion of the decay curves are almost parallel indicates that the survival probability of excited state population of the regular octahedral sites controls the kinetics of the decay. The detailed analysis of the decay kinetics is now in progress.

4. CONCLUSION

The variety of emission lines in the gahnite-like glass-ceramics and the possibility to ascribe these lines to various Cr^{3+} centers can be a useful tool in following the mechanisms of the nucleation of glass-ceramics doped by Cr^{3+}. The high quantum efficiency of Cr^{3+} emission in glass-ceramics and the proximity of $^4T_2$ and ^2E levels

in the distorted sites may have importance in designing tunable lasers.

Acknowledgement: The authors are very grateful to Dr. M. Eyal for fruitful discussions and also to Mr. and Mrs. Willy Berler for their kind support of the work in this laboratory.

REFERENCES

1. R. Reisfeld, Materials Science and Engineering 71 (1985) 375.
2. R. Reisfeld, Potential uses of chromium(III) doped transparent glass-ceramics in luminescent solar concentrators. Rep. Swedish Acad. Engineering Sciences in Finland. No. 40. Proc. Advanced Summer School on Electronic Structure of New Materials, Loviisa, Finland, 1984, Part I (1984) 7.
3. R. Reisfeld, A. Kisilev, E. Greenberg, A. Buch and M. Ish-Shalom, Chem. Phys. Letters 104 (1984) 153.
4. G. Boulon, Energy Transfer Processes in Condensed Matter (ed. B. DiBartolo) Plenum Press (1983) ASI Series - Series B: Physics 114 (1984) 663.
5. M. Bouderbala, G. Boulon, A. Kisilev, R. Reisfeld, A. Buch, M. Ish-Shalom and A.-M. Lejus, Laser spectroscopy of Cr^{3+} in magnesium aluminate spinels and transparent glass-ceramics, to be published.
6. W. Mikenda and A. Preisinger, J. Luminescence, 26 (1981) 53, 67; W. Mikenda, ibid 26 (1981) 85; J. Derkosh and W. Mikenda, ibid 28 (1983) 431.
7. A. Kisilev, R. Reisfeld, A. Buch and M. Ish-Shalom, Transparent glass-ceramics doped by Cr^{3+}: Spectroscopic properties and characterisation of crystalline phases; submitted to Journal of Non-crystalline Solids.

FIGURE CAPTIONS

FIGURE 1. Comparison of the emission spectra of Cr^{3+} in $ZnAl_2O_4$ at λ_{ex} = 532 nm and temperature 4.4 K with Cr^{3+} in gahnite glass-ceramics.

1a. At various excitation wavelengths and temperature 4.4 K.

1b. At λ_{ex} = 532 nm and various temperatures.

FIGURE 2. Excitation spectra of Cr^{3+} in gahnite glass-ceramics at various emission wavelengths at 4.4 K.

FIGURE 3. Time resolved spectra of Cr^{3+} in gahnite glass-ceramics at λ_{ex} = 570 nm, T = 4.4 K.

FIGURE 4. Decay times of Cr^{3+} in

4a A - gahnite glass-ceramics

4b. B and C - $ZnAl_2O_4$

4c. A,B,C - gahnite glass-ceramics.

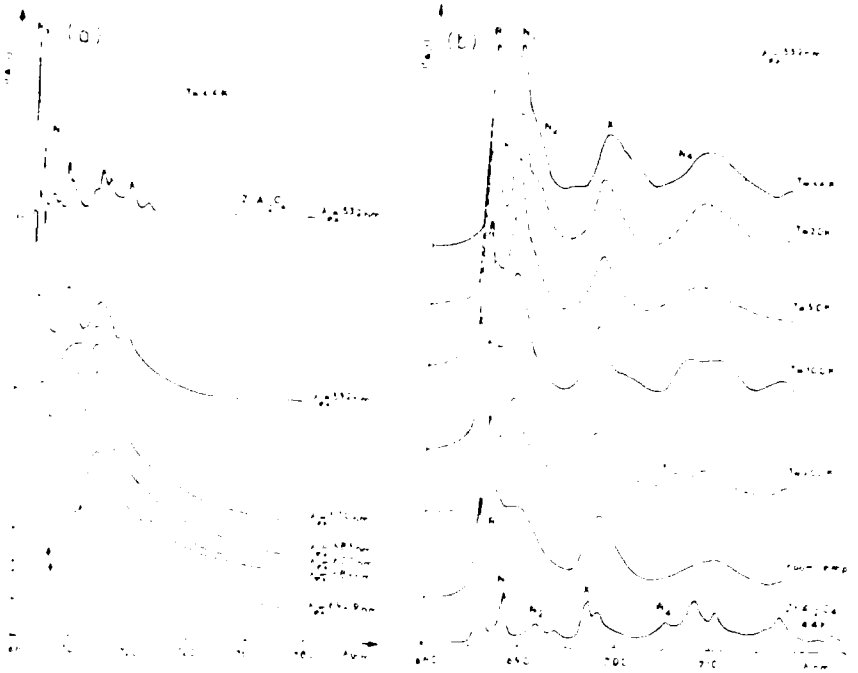

Fig 1.

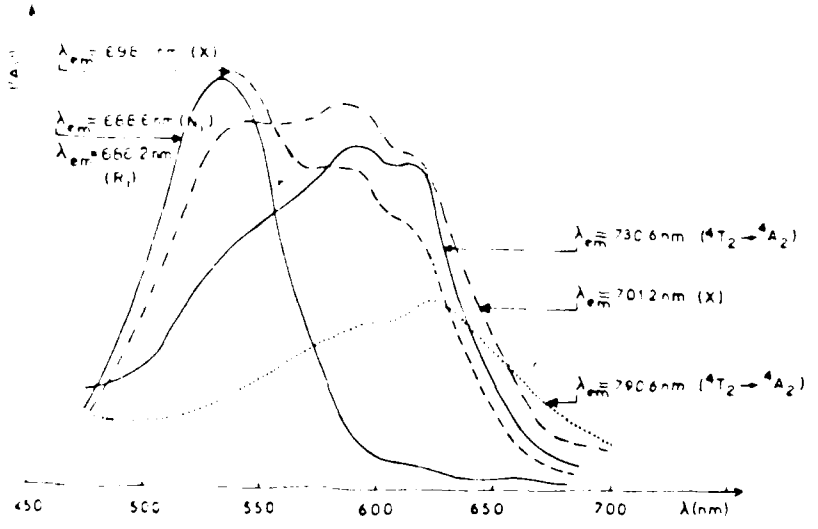
λ_{em} = 696 nm (X)
λ_{em} = 666 nm (R_1)
λ_{em} = 686.2 nm (R_1)
λ_{em} = 730.6 nm ($^4T_2 \rightarrow {}^4A_2$)
λ_{em} = 701.2 nm (X)
λ_{em} = 790.6 nm ($^4T_2 \rightarrow {}^4A_2$)
450
500
550
600
650
700
λ(nm)

Fig 2

Fig 3

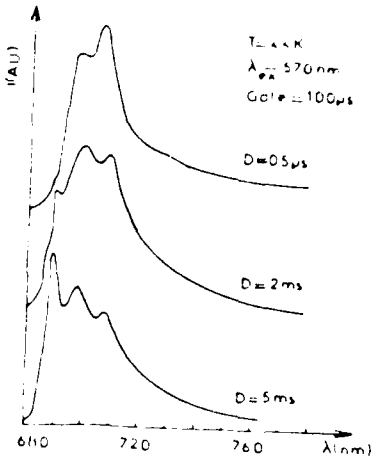
I(A.U.)
T= 4 K
λexc 570 nm
Gate = 100μs
D=0.5μs
D=2ms
D=5ms
640
720
760
λ(nm)

Fig 4

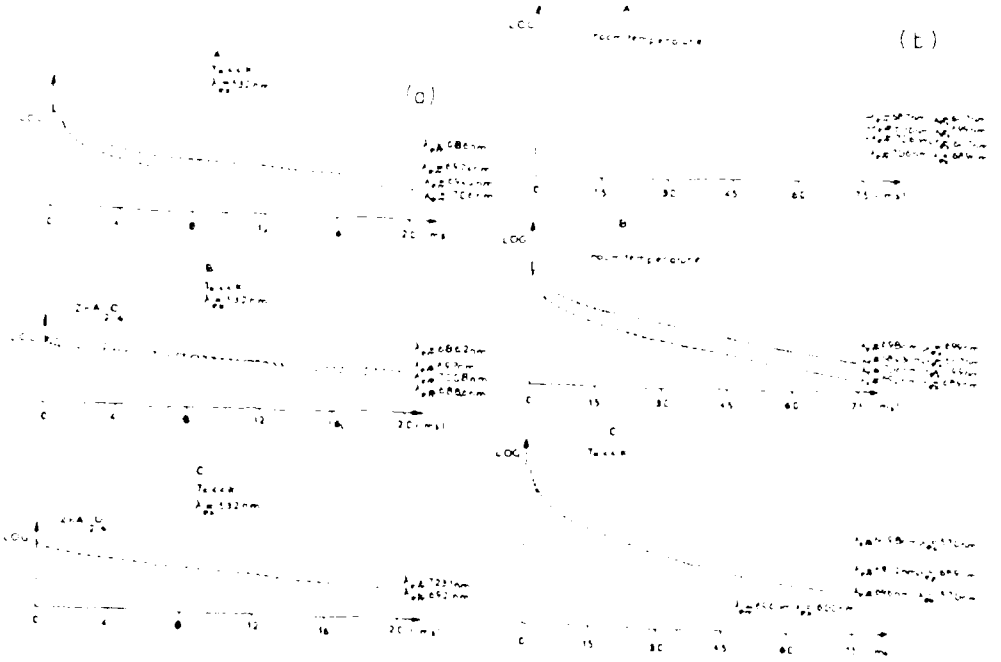
(a)
(b)


FILMED
58